

000 001 002 003 004 005 006 007 008 009 010 011 012 013 014 015 016 017 018 019 020 021 022 023 024 025 026 027 028 029 030 031 032 033 034 035 036 037 038 039 040 041 042 043 044 045 046 047 048 049 050 051 052 053 LEARNING FROM OBSERVATIONAL OUTCOMES: TOWARD CAUSALLY-ALIGNED LANGUAGE MODEL FINE-TUNING

Anonymous authors

Paper under double-blind review

ABSTRACT

Large language models are being widely used across industries to generate text that contributes directly to key performance metrics, such as medication adherence in patient messaging and conversion rates in content generation. Pretrained models, however, often fall short when it comes to aligning with human preferences or optimizing for business objectives. As a result, fine-tuning with good-quality labeled data is essential to guide models to generate content that achieves better results. Controlled experiments, like A/B tests, can provide such data, but they are often expensive and come with significant engineering, logistical, and ethical challenges. Meanwhile, companies have access to a vast amount of historical (observational) data that remains underutilized. In this work, we study the challenges and opportunities of fine-tuning LLMs using observational data. We show that while observational outcomes can provide valuable supervision, directly fine-tuning models on such data can lead them to learn spurious correlations. We present empirical evidence of this issue using various real-world datasets and propose DECONFONDLM, a method that explicitly removes the effect of known confounders from reward signals. In simulation experiments, DECONFONDLM more accurately recovers causal relationships and mitigates failure modes of methods that assume counterfactual invariance, achieving over 16% higher objective score than ODIN and other baselines, when entangled confounding is present.

1 INTRODUCTION

Large language models (LLMs) can be powerful tools for creating content that affects user behavior and supports business goals. From enhancing user engagement to increasing purchase likelihood, companies often aim to generate content that delivers measurable outcomes. Prior research has shown that pretrained LLMs can perform well in certain tasks, such as generating creative product ideas (Castelo et al., 2024) and predicting the likelihood of purchases (Arora et al., 2025). However, these models often struggle to capture human preferences and directly optimize for business outcomes (Goli & Singh, 2024; Ye et al., 2024), emphasizing the need for fine-tuning with labeled data to causally guide the models towards desired business outcomes. Yet obtaining the right kind of labeled data to support this alignment is difficult; human-labeled data and surveys can introduce bias due to artificial contexts (Yeh et al., 2024), and randomized experiments are often infeasible due to logistical and opportunity costs (Quin et al., 2024). This paper explores how to bridge this gap using an abundant but underutilized source of supervision available to firms: historical observational data.

Consider a news website that aims to improve the click-through rates (CTR) of news headlines. While they may not have the capacity to run controlled experiments, they may track how users respond to different headlines over time, which could be used for fine-tuning. However, directly fine-tuning on this data could be challenging because external factors such as time trends may influence both the content and the outcome. Furthermore, while running controlled experiments may already be impractical for a news website, the difficulty is amplified in healthcare settings, where fairness and ethical concerns further restrict experimentation and increase the importance of leveraging available historical data. In this paper, we examine both the opportunities and risks associated with using observational data, and we propose a novel method that corrects for confounding effects in the fine-tuning process.

054 Fine-tuned LLMs have been used in many domains from electronic health records (Wu et al., 2024)
 055 to astronomical data (Wang et al., 2024b) and social-science corpora; however most work does
 056 not discuss causal challenges or the pitfalls of learning from historical data. In business settings,
 057 methods such as Ye et al. (2024) and Angelopoulos et al. (2024) rely on experimental supervision,
 058 leaving the potential of firms’ extensive historical logs underexplored. On the causal side, computer
 059 science work has documented biases in preference data used for fine-tuning (e.g., length bias and
 060 sycophancy) and proposed methods, such as ODIN (Chen et al., 2024), Wang et al. (2025), and Sri-
 061 vastava et al. (2025) that rely on the counterfactual invariance assumption. This assumption forces
 062 the reward estimates not to change when confounding attributes are changed. While counterfac-
 063 tual invariance may be plausible for human-rated LLM outputs, it is often violated in real-world
 064 applications where different variables can affect outcomes. In contrast, we propose a method to use
 065 abundant observational data and correct for observed confounders without assuming counterfactual
 066 invariance.

067 Our results in this paper show:

- 068 • **Risks of observational signals.** Using *StackExchange*, we show that naive fine-tuning on
 069 historical interactions can lead models to internalize spurious correlations.
- 070 • **Value of observational signals.** Using *Upworthy*, we show that observational data can
 071 provide valuable signals. We also highlight the role of regularization to suppress the con-
 072 founding effects when using historical data.
- 073 • **Confounder correction.** We propose DECONFONDLM, a fine-tuning method that re-
 074 moves the influence of observed confounders from the reward signal. Our results show
 075 that this approach consistently improves model behavior, enabling it to focus on causally
 076 relevant attributes rather than superficial artifacts.

079 2 RELATED WORK

081 Our research spans three domains: (1) LLMs in science and business, (2) causal inference in econo-
 082 metrics and machine learning, and (3) alignment of LLMs with reward modeling under confound-
 083 ing. We summarize key contributions in each domain and highlight how our work extends current
 084 boundaries, particularly in aligning LLMs using observational data subject to confounding.

086 2.1 LLMs IN SCIENCE AND BUSINESS APPLICATIONS

088 LLMs have advanced applications across domains, from health records (Wu et al., 2024) and as-
 089 tronomy (Wang et al., 2024b) to social sciences. In business, most work leverages experimental
 090 supervision: Ye et al. (2024) use adaptive experiments for headline CTR, while Angelopoulos et al.
 091 (2024) fine-tune on A/B outcomes. Other efforts explore knowledge transfer (Wang et al., 2024a)
 092 and demand prediction (Lee, 2024). Together, these works highlight the promise of LLMs in busi-
 093 ness settings. However, aside from the last study, which focuses on demand prediction rather than
 094 content generation, these methods primarily rely on supervision signals obtained from controlled ex-
 095 periments, which are costly and limited in scope (Feit & Berman, 2019; Miller & Hosanagar, 2020),
 096 or on synthetic feedback that may reflect the biases of the teacher model. In contrast, our work
 097 investigates how to fine-tune LLMs using abundant observational data, while explicitly addressing
 098 the confounding factors that can mislead model learning.

099 2.2 CAUSAL INFERENCE WITH MACHINE LEARNING AND ECONOMETRICS

101 Econometric methods offer tools for causal learning under confounding. Chernozhukov et al. (2018)
 102 introduce Double Machine Learning (DML), using orthogonalized moment conditions and cross-
 103 fitting to reduce bias from regularization in high-dimensional settings. Farrell et al. (2021) ex-
 104 tend this framework with a theoretical analysis for deep neural networks in semiparametric models.
 105 However, both methods assume exogeneity, limiting their utility when confounding is endogenous.
 106 IV-based approaches (Dikkala et al., 2020; Bennett et al., 2019; Singh & Zheng, 2023) handle endo-
 107 geneity using adversarial or nonparametric estimation. Our work contributes to this line of research
 by adapting IV-based ideas for generative modeling with LLMs. Instead of estimating structural

108 parameters, our goal is to deconfound reward signals used in LLM fine-tuning, ensuring the model
 109 aligns with causal rather than spurious objectives.
 110

111 **2.3 LLM ALIGNMENT AND REWARD MODELING**
 112

113 RLHF has become standard for alignment (Ouyang et al., 2022), with PPO and DPO leveraging
 114 human preference data (Rafailov et al., 2024b; Zheng et al., 2023). Yet reward models inherit bias
 115 (Ntoutsi et al., 2020) and overfit to artifacts like length or sycophancy (Tien et al., 2022; Denison
 116 et al., 2024). To address these issues, several works have developed causal reward modeling frame-
 117 works. However, these methods typically assume counterfactual invariance, that the reward should
 118 not change when confounding attributes are perturbed—an assumption that often fails in practice.
 119 ODIN (Chen et al., 2024) removes known confounders (e.g., length) from the learned reward. Wang
 120 et al. (2025) train rewards to satisfy counterfactual invariance by construction. More recently, Srivastava
 121 et al. (2025) proposes a robust reward modeling method that enforces counterfactual invariance
 122 via counterfactual data augmentation. While the counterfactual invariance assumption may hold
 123 for LLM-generated answers evaluated by humans, it does not hold in many real-world applications,
 124 which we discuss more below.
 125

$$f(\mathbf{F}, \mathbf{C}) = f(\mathbf{F}),$$

127 with \mathbf{F} denoting meaningful features and \mathbf{C} confounders. Approaches like ODIN (Chen et al.,
 128 2024), invariant training (Wang et al., 2025), and augmentation-based methods (Srivastava et al.,
 129 2025) rely on this assumption. However, it is overly restrictive in real-world business contexts where
 130 confounders (e.g., price, seasonality) legitimately affect outcomes. Our method, DECONFONDLM,
 131 relaxes invariance by estimating and removing spurious influences, enabling alignment with true
 132 causal drivers.
 133

134 **3 OBSERVATIONAL DATA: PITFALLS AND POTENTIAL**
 135

136 In this section, we examine both the pitfalls and potential of learning from historical observational
 137 data, relying on experiments using StackExchange and Upworthy data.
 138

139 **3.1 PITFALL: INTERNALIZING SPURIOUS CORRELATION**
 140

141 We illustrate how confounding in historical data can mis-specify rewards when fine-tuning LMs.
 142 Using Academia Stack Exchange, we mimic Askell et al. (2021) by treating user scores as prefer-
 143 ences. In this dataset, engagement varies by weekday, specifically, we see a higher activity earlier
 144 in the week (Figure 1). Because of this pattern, scores partly reflect exposure rather than quality.
 145 To make this spurious signal explicit, we prepend a “Happy Monday!” marker to Monday answers,
 146 then construct preference pairs where the higher-scored answer is treated as preferred. Evaluated
 147 on 3,000 held-out questions, models trained on these preferences learn the weekday cue: compared
 148 to SFT, DPO amplifies the artifact, generating “Happy” 21.2% vs. 13.7% and “Monday” 11.8%
 149 vs. 9.1% of the time (both increases statistically significant). Full description and details of this
 150 experiment are presented in Appendix B.
 151

152 **3.2 POTENTIAL**
 153

154 In the previous section, we showed that historical data can induce spurious correlations. Here we
 155 ask: *What is its potential value?* When a firm lacks experimental data, can logs of content and
 156 observed performance still improve future predictions? This cannot be answered in purely observa-
 157 tional settings because outcomes are not causally attributable to the content. We therefore use the
 158 Upworthy dataset Matias et al. (2021), which provides CTRs from controlled A/B tests. To simulate
 159 observational access, we retain a single headline package and its CTR from each test and discard the
 160 alternative; dataset statistics and preprocessing are discussed in Appendix C.
 161

The realized CTR of a headline package depends not only on its intrinsic appeal but also on exoge-
 162 nous factors such as audience composition and temporal context. For example, surges of sports-
 163 related traffic during major events or elevated engagement with political content during election

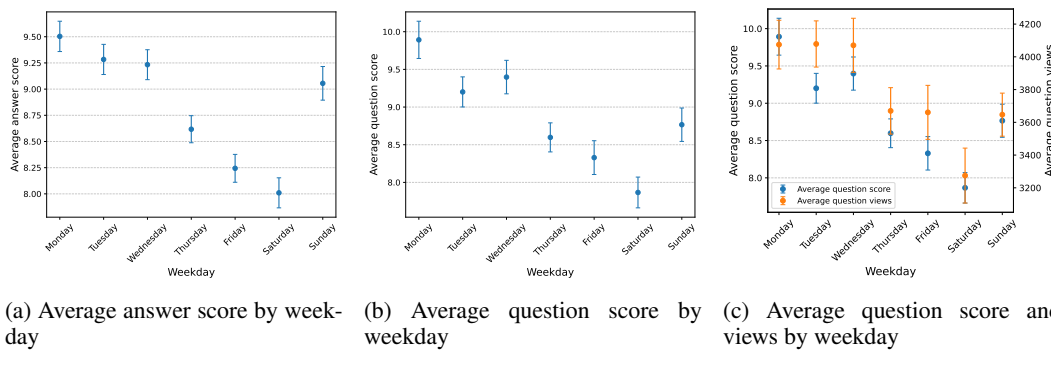


Figure 1: Weekly temporal patterns in Stack Exchange engagement. User scores and views exhibit strong weekday effects, with higher engagement early in the week.

periods can substantially influence observed CTRs. Figure 2a illustrates these dynamics: average CTRs exhibit pronounced temporal variation across experimental training, observational training, and observational validation subsets. Monthly averages are highly correlated across subsets (pairwise correlations of 96–97%), indicating that these fluctuations are systematic rather than stochastic.

These findings raise concerns regarding the direct use of raw CTRs for model training. Temporal shifts in audience composition and preferences may dominate the signal, leading models to capture time-specific artifacts rather than structural attributes of headline quality. Figure 2b provides further evidence, showing substantial variation in impressions per package over time, including a marked increase in late 2023 coinciding with the U.S. election period. Such variation suggests non-stationarity in both traffic volume and audience characteristics. Consequently, models trained naively on observational CTRs risk conflating shifts in exposure and demand with causal effects of content, thereby limiting their ability to generalize beyond the training environment.

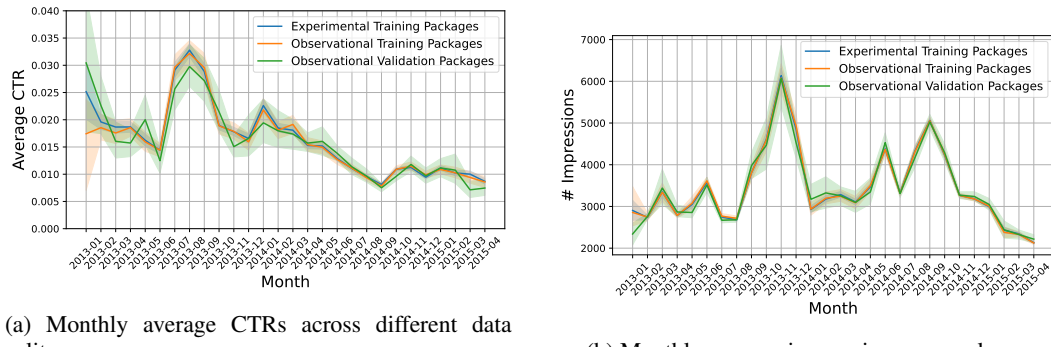
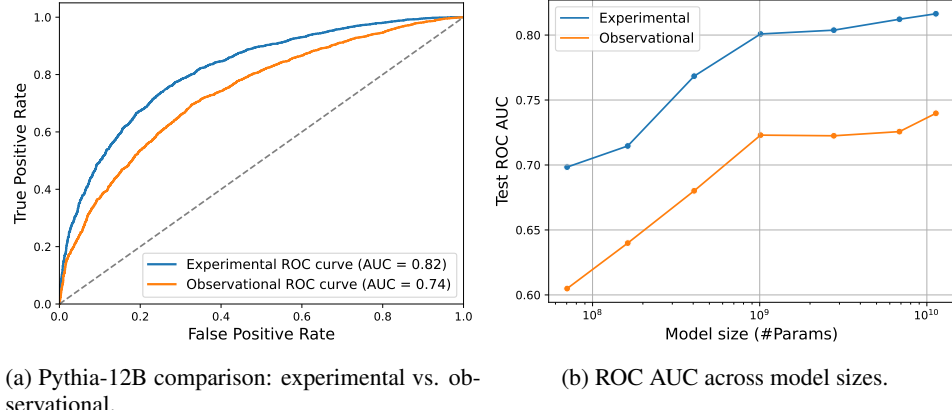


Figure 2: Temporal patterns in user engagement. The left plot shows variation in average click-through rates (CTR) across months, while the right plot shows the number of impressions per package, indicating changes in user traffic volume.

To compare learning from experimental vs. observational data, we fine-tune LLMs by adding a small head to the final embeddings: (i) a pairwise classification head with logistic loss to predict the higher-CTR headline (experimental), and (ii) a regression head with MSE to predict observed CTR (observational). In both settings, we use L_2 regularization and tune λ on a validation set.

Performance. We evaluate all models on the same held-out set of headline pairs, where each pair comes from an A/B test with a known preferred headline. The evaluation objective is to assess whether the model correctly ranks the preferred headline higher. To do this, we compute the ROC AUC (Area Under the Receiver Operating Characteristic Curve), which reflects the model's ability to distinguish between better and worse-performing headlines. We use the Pythia suite of open-weight language models for all experiments Biderman et al. (2023). Figure 3a shows the ROC

AUC results for the Pythia-12B model. Training on the experimental dataset yields an AUC of 0.82, whereas the observational dataset produces a lower, but still above-chance, AUC of 0.74. This result is encouraging: it suggests that historical data, even without experimental variation and with only about 26% of the training packages, can still provide meaningful signals for preference learning. The performance gap also highlights the value of randomized feedback; exposure to counterfactual comparisons enables better generalization and more reliable preference estimation. Figure 3b further shows AUC improves with model size in both settings, yet the experimental–observational gap remains, underscoring the value of randomized feedback when available.



(a) Pythia-12B comparison: experimental vs. observational.

(b) ROC AUC across model sizes.

Figure 3: ROC on held-out Upworthy headline pairs. (a) ROC curves for models trained with experimental data outperform those trained on observational data. (b) Larger models yield better results in both settings, but the performance gap persists.

Importance of regularization. We study the role of regularization in observational learning and find that strong regularization is critical for generalization. As shown in Figures 4b and 4c, optimal validation loss occurs at $\lambda = 18,000$, yet the best test ROC AUC is achieved at $\lambda = 50,000$. This discrepancy suggests that in the presence of confounding factors, tuning hyperparameters solely based on validation loss may not suffice. The model may overfit to patterns influenced by spurious correlations in the validation data, rather than learning features that generalize causally to unseen headline comparisons. Figure 5a shows that this gap holds across model sizes: stronger regularization consistently yields better test performance than what validation loss would suggest. We further find that larger models generally require stronger regularization for optimal test performance. This observation implies that using a fixed regularization setting across models of different sizes is sub-optimal. Figure 5b demonstrates this by plotting test performance against model size under fixed regularization levels. The figure shows a non-monotonic effect, larger models begin to overfit more if regularization is kept constant. These results emphasize the need to scale regularization appropriately with model capacity in order to maintain generalization, which is often overlooked in practice.

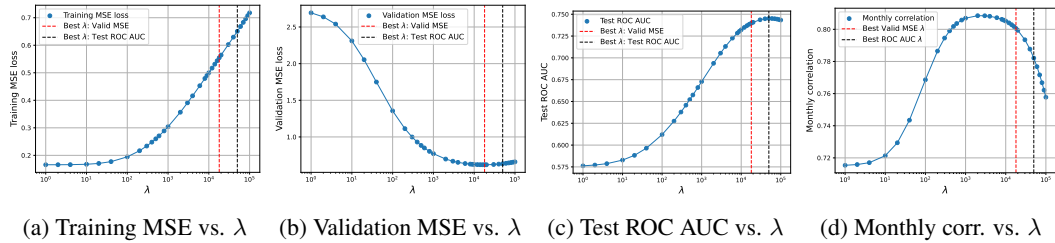


Figure 4: Effect of regularization strength (λ) on different evaluation metrics for the Pythia-12B model.

While these results underscore the critical role of regularization, they also raise a practical challenge when access to held-out experimental data for tuning hyperparameters is often limited. In

such cases, alternative strategies are needed to remove the effect of confounders. We address this issue in Section 4, where we introduce a method for explicitly correcting for confounding effects in observational fine-tuning.

Temporal pattern overfitting. As discussed earlier, temporal variation in CTRs is a potential confounder in observational data. To assess how much models internalize these patterns, we compute the correlation between monthly average CTR estimates on the validation set and observed monthly CTRs in the training data. Figure 4d shows this correlation across values of λ for the Pythia-12B model. We observe that moderate regularization improves alignment with temporal patterns, but higher regularization reduces it. Interestingly, the λ that yields the best test performance comes well after this drop, indicating that suppressing temporal patterns helps the model on the causal evaluation of headlines. This trend holds across model sizes. As shown in Figure 5c, models consistently show lower temporal correlation at their optimal test-time λ , further suggesting that failing to effectively account for confounding patterns can impair generalization performance.

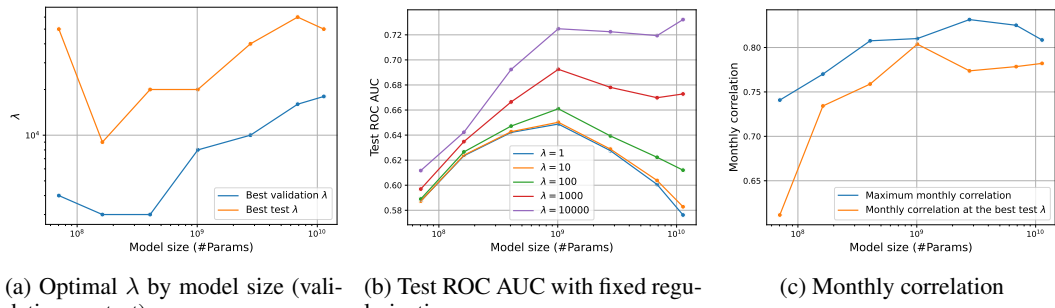


Figure 5: Regularization dynamics across model sizes. (a) Models require larger regularization to achieve optimal test performance. (b) Using a fixed regularization setting leads to non-monotonic scaling performance. (c) Models show lower correlation with temporal engagement patterns at their optimal test-time λ .

4 A CAUSAL FRAMEWORK FOR OBSERVATIONAL FINE-TUNING

We now introduce a formal framework to analyze the effect of confounding in observational fine-tuning. Suppose we have access to historical interaction data $\mathcal{D} = \{(X_i, y_i)\}_{i \in \mathcal{I}}$, where X_i denotes the context vector for interaction i and y_i is the associated outcome (e.g., click-through rate or reservation rate). We assume that X_i can be decomposed into a textual decision variable T_i (e.g., a generated title or headline) and auxiliary features \tilde{X}_i , such that: $y_i = f(T_i, \tilde{X}_i) + \epsilon_i$, where f is the unknown outcome function and ϵ_i is zero-mean noise. The goal is to train a generative model $G : \tilde{X} \rightarrow T$ that produces high-reward textual actions for new inputs. To capture confounding, we assume that the outcome function can be decomposed as:

$$y_i = g(T_i, \tilde{F}_i) + h(C_i) + \epsilon_i, \quad (1)$$

where \tilde{F}_i is the set of observed features including T_i , and C_i represents observed confounders that influence both the action and the outcome. The function g captures the causal effect of the textual action and other features, while h captures the contribution of confounders. Crucially, if g and h are entangled, estimating them independently may result in biased models and reward misspecification.

Proposed method: DECONFOUNDLM Our proposed approach, Deconfounded Language Model Fine-Tuning (DECONFOUNDLM), involves first identifying and modeling the effect of confounders, and then explicitly removing their contribution from the observed outcomes. This allows the model to learn the causal impact of the textual input and other features, without being influenced by confounding effects. In our experiments, we apply an instrumental variable strategy to estimate the confounding component. However, the framework is flexible: other methods such as Double Machine Learning Chernozhukov et al. (2018) or Adversarial GMMs Dikkala et al. (2020) can be used,

324 provided the researcher is mindful of the assumptions of the methods. We further discuss the potential
 325 impacts and limitations in Appendix E.

326 **Example 1** (Partially Linear Regression). Consider a partially linear model where the confounder
 327 p_i , e.g., the price in Airbnb listings, enters linearly (Similar to the examples from Chernozhukov
 328 et al. (2018)):

$$330 \quad y_i = g(T_i, \tilde{\mathbf{F}}_i) + \alpha p_i + \epsilon_i, \quad (2)$$

332 Here, $p_i \in \mathbf{C}_i$ is an observed confounder. In the Airbnb example, when optimizing titles to improve
 333 reservation rates, price may strongly affect y_i and also correlate with certain title patterns (e.g.,
 334 “affordable”). Estimating g accurately thus requires adjusting for p_i to avoid spurious correlations.

336 4.1 SIMULATION EXPERIMENTS

338 In this section, we turn to simulation experiments for a controlled evaluation of the proposed DE-
 339 CONFOUNDLM method. We base our simulation experiments on the MIND dataset (Wu et al.,
 340 2020), which contains over 160,000 English-language news articles with both titles and full text.
 341 We treat the article body as the input context and aim to generate a headline T_i that maximizes a
 342 synthetic performance score y_i , interpreted as a proxy for engagement or click-through rate. To
 343 simulate realistic challenges in observational fine-tuning, we design two scenarios, *Orthogonal con-*
 344 *founding* and *Entangled confounding*, where the observed outcome y_i depends on both the textual
 345 quality and a confounding variable p_i representing topic popularity (e.g., how much fan interest a
 346 team garners). We use the headline sentiment $s(T_i) = g(T_i, \tilde{\mathbf{F}}_i)$ as a measure of quality, as it is
 347 interpretable and easily measured.

348 Across both scenarios, we model the outcome as:

$$350 \quad y_i = s(T_i) + 0.1 p_i + \nu_i, \quad (3)$$

352 where p_i is the confounder, and $\nu_i \sim \mathcal{N}(0, 0.1)$ represents observational noise. We vary how p_i is
 353 constructed across two settings:

- 354 • *Orthogonal confounding*. The confounder p_i is independent of the sentiment $s(T_i)$, making
 355 its effect easier to isolate and remove. Specifically:

$$357 \quad p_i = \mathbb{1}(\text{title mentions West Coast team}) + 2 \cdot \mathbb{1}(\text{Central team}) + 3 \cdot \mathbb{1}(\text{East Coast team}) + \epsilon_i, \quad (4)$$

359 where $\epsilon_i \sim \mathcal{N}(0, 0.5)$. This reflects a hypothetical bias where East Coast teams are gener-
 360 ally more popular and draw higher engagement regardless of the title’s quality.

- 361 • *Entangled confounding*. Here, popularity p_i is correlated with the sentiment of the news
 362 abstract, mimicking a setting where emotional salience of the topic and engagement co-
 363 vary. For instance, sad events may draw more audience to the platform and lead to increased
 364 engagement. We model this with:

$$365 \quad p_i = \mathbb{1}(\text{title mentions West Coast team}) + 2 \cdot \mathbb{1}(\text{Central team}) + 3 \cdot \mathbb{1}(\text{East Coast team}) \\ 366 \quad - 10.5 \cdot s(\text{abstract}) + \epsilon_i. \quad (5)$$

369 **IV justification.** In this setting, both the abstract sentiment $s(\text{abs})$ and team mentions influence
 370 the latent popularity measure p_i , which in turn drives engagement Y_i . Omitting popularity from the
 371 analysis induces bias in the estimated effect of headline sentiment on Y_i , since part of the observed
 372 variation in engagement is mediated by shifts in audience composition or topical salience. Instru-
 373 mental variables (IV) address this problem by exploiting variation that affects the outcome only
 374 through its impact on popularity. In our case, team mentions satisfy this requirement: they generate
 375 exogenous shocks to popularity (e.g., attention surges around specific sporting events) but do not
 376 otherwise alter the causal path from headline sentiment to engagement.

377 The IV procedure estimates and removes the contribution of popularity, leaving only the compo-
 378 nent of engagement that is causally attributable to headline sentiment. This illustrates the classical

378 conditions under which IV estimation is effective: (i) *relevance*, since team mentions are strongly
 379 correlated with popularity, and (ii) *exclusion*, since they affect engagement only through popularity.
 380 When these conditions are satisfied, IV recovers the true causal effect of headline sentiment even in
 381 the presence of confounding.
 382

383 **Comparative methods.** We evaluate seven approaches: (1) a base pre-trained model, (2) super-
 384 vised fine-tuning (SFT), (3) RL with access to ground-truth sentiment (which serves as a baseline)
 385 (4) RL using observed performance without controlling for confounders, (5) RL models that in-
 386 incorporate popularity either as input text or as a scalar feature in the final layer, (6) ODIN (Chen
 387 et al., 2024) as an example of a method that relies on counterfactual invariance, and (7) our pro-
 388 posed method DECONFONDLM-IV, which estimates and removes the confounder effect using an
 389 instrumental variable.
 390

391 **Results.** We evaluate all models’ generations after the RL step on a held-out set of 3,000 news
 392 articles. Table 1 summarizes the average sentiment of generated headlines and the frequency of
 393 team name mentions, which serve as a proxy for reliance on the popularity-based confounder. In the
 394 *Orthogonal* setting, the model trained on observed performance (without accounting for confounding)
 395 is able to improve headline sentiment, indicating that it learns part of the true signal. However,
 396 it also shows a marked increase in the frequency of team name mentions, suggesting reliance on
 397 popularity cues. Incorporating popularity information, either via text prompts or as an input feature,
 398 reduces this effect. Among all methods, DECONFONDLM-IV more closely matches the sentiment
 399 gains of the true-reward model while not generating unnecessary references to team names caused
 400 by the confounding variable.
 401

402 Table 1: Comparison of models under two confounding scenarios. The table reports the mean
 403 sentiments and the number of generated titles mentioning teams by region. Models are tested on
 404 3,000 headline generations. Note that the reported results for the first four models are identical
 405 across both scenarios, as they do not rely on the observed performances; the difference between the
 406 two scenarios lies solely in how the observed performance is constructed.
 407

Model	Scenario 1: Orthogonal				Scenario 2: Entangled			
	Sent.	W	C	E	Sent.	W	C	E
Base Pre-Trained Model	0.684	177	795	717	0.450	177	795	717
SFT Model	0.716	159	634	610	0.716	159	634	610
Model with only sentiment	0.950	165	714	728	0.960	187	697	720
Model with sentiment + noise	0.934	172	699	664	0.958	174	716	699
RL w/ observed performance	0.956	214	914	1016	0.735	186	908	1041
RL w/ pop. in text	0.932	158	655	638	0.718	166	676	629
RL w/ pop. in layer	0.935	178	679	661	0.800	189	829	835
ODIN (Chen et al., 2024)	0.934	178	729	680	0.807	249	1018	1063
DECONFONDLM-IV	0.939	181	692	682	0.937	170	736	694

419 The *Entangled* case presents a more challenging scenario. Here, the naive model trained on observed
 420 performance fails to improve sentiment and heavily generates team names. While models that in-
 421 clude popularity in the input text or final layer performed well in the *orthogonal* setting, they struggle
 422 to recover the sentiment-performance relationship in this setting. ODIN also achieves a similar per-
 423 formance in terms of sentiments of the generated headlines, but generates many more team names.
 424 In contrast, DECONFONDLM-IV demonstrates strong robustness. It successfully suppresses the
 425 influence of the confounder and generates headlines with **16%** higher sentiment scores compared
 426 to the next highest sentiment scores. Full experimental details for the simulation experiments are
 427 provided in Appendix D.
 428

429 **Reward-sentiment correlation.** We now turn to the question of why DECONFONDLM delivers
 430 stronger results: How closely do the reward models actually follow the true sentiment measures?
 431 Table 2 shows the average Pearson correlation between predicted rewards and sentiment scores
 432 in the reward validation set, under two confounding scenarios. In the orthogonal case, observed

432 performance is positively correlated with sentiment, allowing most models to achieve a positive
 433 correlation between their reward estimates and sentiment. However, in the entangled case, where
 434 the confounder (e.g., team popularity) effect is entangled with the outcome, this relationship breaks
 435 down. Most of the models that do not account for the confounder, or attempt to include it through
 436 text features or final-layer embeddings, fail to maintain a positive correlation between predicted
 437 rewards and sentiment. In contrast, DECONFONDLM-IV remains robust across both scenarios,
 438 maintaining a strong positive correlation.

439
 440 Table 2: Correlation between predicted rewards and sentiment across two confounding scenarios.
 441 Each cell shows the Pearson correlation on the train and validation sets. The reported results for
 442 the first two models are identical across both scenarios, as they do not rely on the observed perfor-
 443 mances.

445 446 447 448 449 450 451 452 453 454 455 456 457 458 459 460 461 462 463 464 465 466 467 468 469 470 471 472 473 474 475 476 477 478 479 480 481 482 483 484 485	445 446 447 448 449 450 451 452 453 454 455 456 457 458 459 460 461 462 463 464 465 466 467 468 469 470 471 472 473 474 475 476 477 478 479 480 481 482 483 484 485	445 446 447 448 449 450 451 452 453 454 455 456 457 458 459 460 461 462 463 464 465 466 467 468 469 470 471 472 473 474 475 476 477 478 479 480 481 482 483 484 485		445 446 447 448 449 450 451 452 453 454 455 456 457 458 459 460 461 462 463 464 465 466 467 468 469 470 471 472 473 474 475 476 477 478 479 480 481 482 483 484 485	
		445 446 447 448 449 450 451 452 453 454 455 456 457 458 459 460 461 462 463 464 465 466 467 468 469 470 471 472 473 474 475 476 477 478 479 480 481 482 483 484 485	445 446 447 448 449 450 451 452 453 454 455 456 457 458 459 460 461 462 463 464 465 466 467 468 469 470 471 472 473 474 475 476 477 478 479 480 481 482 483 484 485	445 446 447 448 449 450 451 452 453 454 455 456 457 458 459 460 461 462 463 464 465 466 467 468 469 470 471 472 473 474 475 476 477 478 479 480 481 482 483 484 485	445 446 447 448 449 450 451 452 453 454 455 456 457 458 459 460 461 462 463 464 465 466 467 468 469 470 471 472 473 474 475 476 477 478 479 480 481 482 483 484 485
Model		Scenario 1: Orthogonal Train	Scenario 1: Orthogonal Valid	Scenario 2: Entangled Train	Scenario 2: Entangled Valid
Model with only sentiment	0.913	0.872	0.913	0.872	
Model with sentiment + noise	0.910	0.891	0.807	0.802	
RL w/ observed performance	0.880	0.859	-0.073	-0.079	
RL w/ pop. in text	0.839	0.827	-0.261	-0.253	
RL w/ pop. in layer	0.862	0.841	0.623	0.627	
ODIN Chen et al. (2024)	0.654	0.641	-0.536	-0.542	
DECONFONDLM-IV	0.915	0.886	0.898	0.867	

5 CONCLUSION AND DISCUSSION

Our findings suggest that using historical data to fine-tune language models can be a double-edged sword: while it provides valuable information without the need for experimentation, it could also introduce the risk of learning from confounded outcomes. Through both real-world and synthetic experiments, we show that models trained on observational data may internalize spurious correlations that are not causally linked to content quality. To mitigate this, we introduce DECONFONDLM, a method that explicitly adjusts for observed confounders in the fine-tuning process. By separating confounding influences from the outcome signal, our approach enables more causally grounded learning without relying on the counterfactual invariance assumption that is often used in prior work. Across multiple settings, we find that DECONFONDLM improves fine-tuning outcomes and better captures the true effects of textual inputs. Finally, while our primary focus is performance and causal inference, we note that confounding can also introduce fairness concerns. If unaddressed, it may lead models to replicate or amplify structural biases in the data. We view causal deconfounding as a promising direction for aligning language models not only with user preferences but also with broader values of equity and accountability.

REFERENCES

Loubna Ben Allal, Anton Lozhkov, Elie Bakouch, Gabriel Martín Blázquez, Guilherme Penedo, Lewis Tunstall, Andrés Marafioti, Hynek Kydlíček, Agustín Piqueres Lajarín, Vaibhav Srivastav, Joshua Lochner, Caleb Fahlgren, Xuan-Son Nguyen, Clémentine Fourrier, Ben Burtenshaw, Hugo Larcher, Haojun Zhao, Cyril Zakka, Mathieu Morlon, Colin Raffel, Leandro von Werra, and Thomas Wolf. Smollm2: When smol goes big – data-centric training of a small language model, 2025. URL <https://arxiv.org/abs/2502.02737>.

Panagiotis Angelopoulos, Kevin Lee, and Sanjog Misra. Causal alignment: Augmenting language models with a/b tests. *Available at SSRN*, 2024.

Neeraj Arora, Ishita Chakraborty, and Yohei Nishimura. Ai–human hybrids for marketing research: Leveraging large language models (llms) as collaborators. *Journal of Marketing*, 89(2):43–70, 2025.

486 Amanda Askell, Yuntao Bai, Anna Chen, Dawn Drain, Deep Ganguli, Tom Henighan, Andy Jones,
 487 Nicholas Joseph, Ben Mann, Nova DasSarma, et al. A general language assistant as a laboratory
 488 for alignment. *arXiv preprint arXiv:2112.00861*, 2021.

489 Andrew Bennett, Nathan Kallus, and Tobias Schnabel. Deep generalized method of moments for
 490 instrumental variable analysis. *Advances in neural information processing systems*, 32, 2019.

492 Stella Biderman, Hailey Schoelkopf, Quentin Gregory Anthony, Herbie Bradley, Kyle O'Brien, Eric
 493 Hallahan, Mohammad Aflah Khan, Shivanshu Purohit, USVSN Sai Prashanth, Edward Raff, et al.
 494 Pythia: A suite for analyzing large language models across training and scaling. In *International
 495 Conference on Machine Learning*, pp. 2397–2430. PMLR, 2023.

496 Noah Castelo, Zsolt Katona, Peiyao Li, and Miklos Sarvary. How ai outperforms humans at creative
 497 idea generation. *Available at SSRN 4751779*, 2024.

499 Lichang Chen, Chen Zhu, Davit Soselia, Juhai Chen, Tianyi Zhou, Tom Goldstein, Heng Huang,
 500 Mohammad Shoeybi, and Bryan Catanzaro. Odin: Disentangled reward mitigates hacking in rlhf.
 501 *arXiv preprint arXiv:2402.07319*, 2024.

502 Victor Chernozhukov, Denis Chetverikov, Mert Demirer, Esther Duflo, Christian Hansen, Whitney
 503 Newey, and James Robins. Double/debiased machine learning for treatment and structural pa-
 504 rameters. *The Econometrics Journal*, 21(1):C1–C68, 2018.

506 Carson Denison, Monte MacDiarmid, Fazl Barez, David Duvenaud, Shauna Kravec, Samuel Marks,
 507 Nicholas Schiefer, Ryan Soklaski, Alex Tamkin, Jared Kaplan, et al. Sycophancy to subterfuge:
 508 Investigating reward-tampering in large language models. *arXiv preprint arXiv:2406.10162*,
 509 2024.

510 Nishanth Dikkala, Greg Lewis, Lester Mackey, and Vasilis Syrgkanis. Minimax estimation of con-
 511 ditional moment models. *Advances in Neural Information Processing Systems*, 33:12248–12262,
 512 2020.

513 Jianqing Fan and Yuan Liao. Endogeneity in high dimensions. *Annals of statistics*, 42(3):872, 2014.

515 Max H Farrell, Tengyuan Liang, and Sanjog Misra. Deep neural networks for estimation and infer-
 516 ence. *Econometrica*, 89(1):181–213, 2021.

517 Elea McDonnell Feit and Ron Berman. Test & roll: Profit-maximizing a/b tests. *Marketing Science*,
 518 38(6):1038–1058, 2019.

520 Leo Gao, John Schulman, and Jacob Hilton. Scaling laws for reward model overoptimization. In
 521 *International Conference on Machine Learning*, pp. 10835–10866. PMLR, 2023.

522 Ali Goli and Amandeep Singh. Frontiers: Can large language models capture human preferences?
 523 *Marketing Science*, 43(4):709–722, 2024.

525 Daya Guo, Dejian Yang, Haowei Zhang, Junxiao Song, Ruoyu Zhang, Runxin Xu, Qihao Zhu,
 526 Shirong Ma, Peiyi Wang, Xiao Bi, et al. Deepseek-r1: Incentivizing reasoning capability in llms
 527 via reinforcement learning. *arXiv preprint arXiv:2501.12948*, 2025.

528 Edward J Hu, Yelong Shen, Phillip Wallis, Zeyuan Allen-Zhu, Yuanzhi Li, Shean Wang, Lu Wang,
 529 Weizhu Chen, et al. Lora: Low-rank adaptation of large language models. *ICLR*, 1(2):3, 2022.

531 Harrison Lee, Samrat Phatale, Hassan Mansoor, Kellie Ren Lu, Thomas Mesnard, Johan Ferret,
 532 Colton Bishop, Ethan Hall, Victor Carbune, and Abhinav Rastogi. RLAIF: Scaling reinforcement
 533 learning from human feedback with AI feedback, 2024. URL <https://openreview.net/forum?id=AAxIs3D2Z>.

535 Kevin Lee. Generative brand choice. Technical report, Working Paper, 2024.

536 J Nathan Matias, Kevin Munger, Marianne Aubin Le Quere, and Charles Ebersole. The upworthy
 537 research archive, a time series of 32,487 experiments in us media. *Scientific Data*, 8(1):195, 2021.

539 Ninareh Mehrabi, Fred Morstatter, Nripsuta Saxena, Kristina Lerman, and Aram Galstyan. A survey
 on bias and fairness in machine learning. *ACM computing surveys (CSUR)*, 54(6):1–35, 2021.

540 Alex P Miller and Kartik Hosanagar. An empirical meta-analysis of e-commerce a/b testing strate-
 541 gies. *The Wharton School, University of Pennsylvania*, 2020.

542

543 Eirini Ntoutsi, Pavlos Fafalios, Ujwal Gadiraju, Vasileios Iosifidis, Wolfgang Nejdl, Maria-Esther
 544 Vidal, Salvatore Ruggieri, Franco Turini, Symeon Papadopoulos, Emmanouil Krasanakis, et al.
 545 Bias in data-driven artificial intelligence systems—an introductory survey. *Wiley Interdisciplinary
 546 Reviews: Data Mining and Knowledge Discovery*, 10(3):e1356, 2020.

547

548 Long Ouyang, Jeffrey Wu, Xu Jiang, Diogo Almeida, Carroll Wainwright, Pamela Mishkin, Chong
 549 Zhang, Sandhini Agarwal, Katarina Slama, Alex Ray, et al. Training language models to fol-
 550 low instructions with human feedback. *Advances in neural information processing systems*, 35:
 27730–27744, 2022.

551

552 Federico Quin, Danny Weyns, Matthias Galster, and Camila Costa Silva. A/b testing: A systematic
 553 literature review. *Journal of Systems and Software*, pp. 112011, 2024.

554

555 Rafael Rafailov, Yaswanth Chittepu, Ryan Park, Harshit Sushil Sikchi, Joey Hejna, Brad Knox,
 556 Chelsea Finn, and Scott Niekum. Scaling laws for reward model overoptimization in direct
 557 alignment algorithms. *Advances in Neural Information Processing Systems*, 37:126207–126242,
 2024a.

558

559 Rafael Rafailov, Archit Sharma, Eric Mitchell, Christopher D Manning, Stefano Ermon, and Chelsea
 560 Finn. Direct preference optimization: Your language model is secretly a reward model. *Advances
 561 in Neural Information Processing Systems*, 36, 2024b.

562

563 Amandeep Singh and Bolong Zheng. Causal regressions for unstructured data. In *Causal Repre-
 564 sentation Learning Workshop at NeurIPS 2023*, 2023. URL [https://openreview.net/
 forum?id=Zs3C7zytfp](https://openreview.net/forum?id=Zs3C7zytfp).

565

566 Pragya Srivastava, Harman Singh, Rahul Madhavan, Gandharv Patil, Sravanti Addepalli, Arun Sug-
 567 gala, Rengarajan Aravamudhan, Soumya Sharma, Anirban Laha, Aravindan Raghuveer, et al.
 568 Robust reward modeling via causal rubrics. *arXiv preprint arXiv:2506.16507*, 2025.

569

570 Jeremy Tien, Jerry Zhi-Yang He, Zackory Erickson, Anca D Dragan, and Daniel S Brown. Causal
 571 confusion and reward misidentification in preference-based reward learning. *arXiv preprint
 572 arXiv:2204.06601*, 2022.

573

574 Chaoqi Wang, Zhuokai Zhao, Yibo Jiang, Zhaorun Chen, Chen Zhu, Yuxin Chen, Jiayi Liu, Lizhu
 575 Zhang, Xiangjun Fan, Hao Ma, et al. Beyond reward hacking: Causal rewards for large language
 576 model alignment. *arXiv preprint arXiv:2501.09620*, 2025.

577

578 Tong Wang, K Sudhir, and Dat Hong. Using advanced llms to enhance smaller llms: An interpretable
 579 knowledge distillation approach. *arXiv preprint arXiv:2408.07238*, 2024a.

580

581 Yu Wang, Shu-Rui Zhang, Aidin Momtaz, Rahim Moradi, Fatemeh Rastegarnia, Narek Sahakyan,
 582 Soroush Shakeri, and Liang Li. Can ai understand our universe? test of fine-tuning gpt by astro-
 583 physical data. *arXiv preprint arXiv:2404.10019*, 2024b.

584

585 Fangzhao Wu, Ying Qiao, Jiun-Hung Chen, Chuhan Wu, Tao Qi, Jianxun Lian, Danyang Liu, Xing
 586 Xie, Jianfeng Gao, Winnie Wu, et al. Mind: A large-scale dataset for news recommendation.
 587 In *Proceedings of the 58th annual meeting of the association for computational linguistics*, pp.
 588 3597–3606, 2020.

589

590 Zhenbang Wu, Anant Dadu, Mike Nalls, Faraz Faghri, and Jimeng Sun. Instruction tuning
 591 large language models to understand electronic health records. In A. Globerson, L. Mackey,
 592 D. Belgrave, A. Fan, U. Paquet, J. Tomczak, and C. Zhang (eds.), *Advances in Neural In-
 593 formation Processing Systems*, volume 37, pp. 54772–54786. Curran Associates, Inc., 2024.
 594 URL https://proceedings.neurips.cc/paper_files/paper/2024/file/62986e0a78780fe5f17b495aeded5bab-Paper-Datasets_and_Benchmarks_Track.pdf.

595

596 Zikun Ye, Hema Yoganarasimhan, and Yufeng Zheng. Lola: Llm-assisted online learning algorithm
 597 for content experiments. *arXiv preprint arXiv:2406.02611*, 2024.

594 Min-Hsuan Yeh, Leitian Tao, Jeffrey Wang, Xuefeng Du, and Yixuan Li. How reliable is human
 595 feedback for aligning large language models? *arXiv preprint arXiv:2410.01957*, 2024.

596
 597 Lik Xun Yuan. distilbert-base-multilingual-cased-sentiments-student (revision
 598 2e33845), 2023. URL <https://huggingface.co/lxyuan/distilbert-base-multilingual-cased-sentiments-student>.

600 Rui Zheng, Shihan Dou, Songyang Gao, Yuan Hua, Wei Shen, Binghai Wang, Yan Liu, Senjie Jin,
 601 Qin Liu, Yuhao Zhou, et al. Secrets of rlhf in large language models part i: Ppo. *arXiv preprint*
 602 *arXiv:2307.04964*, 2023.

603 Daniel M Ziegler, Nisan Stiennon, Jeffrey Wu, Tom B Brown, Alec Radford, Dario Amodei, Paul
 604 Christiano, and Geoffrey Irving. Fine-tuning language models from human preferences. *arXiv*
 605 *preprint arXiv:1909.08593*, 2019.

606 Hui Zou and Hao Helen Zhang. On the adaptive elastic-net with a diverging number of parameters.
 607 *Annals of statistics*, 37(4):1733, 2009.

610 A PROBLEM SETUP AND BACKGROUND

612 Fine-tuning LLMs to align their outputs with user preferences is a common approach for enhancing
 613 their performance. This process typically relies on *labeled preference data*, which may be collected
 614 through human annotations Ziegler et al. (2019), automated feedback mechanisms (e.g., RLAIF Lee
 615 et al. (2024)), or structured reasoning tasks (e.g., Guo et al. (2025)). Two major paradigms are
 616 commonly used to incorporate preference data into LLM training: (i) Reward Modeling followed
 617 by Reinforcement Learning, and (ii) Direct Preference Optimization.

618 In the former, a reward model $r_\phi(x, y)$ is first trained to predict human preferences between outputs
 619 given an input x . The model is typically trained using pairwise comparisons, optimizing a Bradley-
 620 Terry likelihood:

$$621 \quad \mathcal{L}_{\text{RM}}(\phi) = -\mathbb{E}_{(x, y_w, y_l) \sim \mathcal{D}} [\log \sigma(r_\phi(x, y_w) - r_\phi(x, y_l))],$$

623 where σ is the logistic sigmoid. Once trained, this reward model is used to fine-tune the language
 624 model $\pi_\theta(y \mid x)$ using reinforcement learning algorithms such as Proximal Policy Optimization
 625 (PPO), which maximize expected reward while regularizing against a reference policy:

$$626 \quad \max_{\pi_\theta} \mathbb{E}_{x \sim \mathcal{D}, y \sim \pi_\theta(\cdot \mid x)} [r_\phi(x, y) - \beta \text{KL}(\pi_\theta(\cdot \mid x) \parallel \pi_{\text{ref}}(\cdot \mid x))].$$

628 In contrast, *Direct Preference Optimization (DPO)* bypasses reward modeling entirely and directly
 629 updates the policy to prefer higher-rated responses using a contrastive objective over preference
 630 pairs Rafailov et al. (2024b).

632 In industrial applications such as optimizing click-through rates for headlines, boosting booking
 633 rates on rental platforms, or improving adherence in health messaging, the gold standard for eval-
 634 uating outcomes is randomized controlled trials, which allow unbiased estimation of causal effects.
 635 However, such experiments are expensive and often infeasible in practice. Meanwhile, organizations
 636 often have abundant *observational data*: historical logs of content such as page titles, messages, or
 637 headlines and their associated outcomes. This data can be used directly for fine-tuning, either by
 638 training a reward model or by constructing preference pairs for methods like DPO. The challenge,
 639 however, is that observational data is subject to confounding: unobserved variables may influence
 640 both the textual content and the observed outcome, leading to spurious correlations. For exam-
 641 ple, consider an LLM deployed at Airbnb to generate listing titles aimed at increasing reservation
 642 rates. Historical data may show that listings with the word “*affordable*” in the title perform better.
 643 However, this could reflect the underlying confounding effect of the price, as lower-priced listings
 644 generally get higher reservations. A model fine-tuned naively on this data may learn to associate
 645 “*affordable*” with success in all contexts, leading to unsuitable generations. Say you are asking the
 646 model to generate a title for a luxury riverside property, and the model generates ‘‘Affordable
 647 log chalet { perfect for solo travelers’’!

648 This is a clear instance of reward misspecification: the model learns to optimize a proxy signal that
 649 only partially reflects the true objective. While prior work Gao et al. (2023); Rafailov et al. (2024a)

648 has investigated reward over-optimization in both classical RLHF and Direct Alignment settings,
 649 these studies have largely focused on empirical scaling behavior and optimization dynamics. In this
 650 work, we take a step further by analyzing the role of confounding and causal misalignment in fine-
 651 tuning large language models using observational data. In the following section, we investigate how
 652 relying on historical preference data can lead to biased and potentially flawed model fine-tuning, by
 653 examining a real-world case study.

654

655

656 B THE MONDAY EXPERIMENT: AN EXAMPLE OF CONFOUNDER IN 657 OBSERVATIONAL DATA

658

660 In this section, we present an example illustrating how confounding can lead to reward misspecifi-
 661 cation when fine-tuning language models using historical data. Specifically, we construct a dataset
 662 similar to that used by Askell et al. (2021), based on data from the Academia Stack Exchange. In
 663 their study, the authors fine-tune a question-answering model and, in one step of their fine-tuning,
 664 Preference Model Pre-Training (PMP), use historical data to guide learning. They treat answer
 665 scores as preference signals and train the model to prefer higher-scored answers in cases where mul-
 666 tiple answers are available for a question. This PMP step is followed by fine-tuning with human
 667 feedback, to ensure the alignment of the model’s preferences with human judgments. In our experi-
 668 ment, we investigate what happens when human feedback is unavailable and only observational data
 669 is used for fine-tuning.

670 While using the scores can signal which answer is more helpful, these scores are not the outcomes
 671 of randomized experiments, rather could be affected by user engagement patterns. For example,
 672 answers posted earlier may receive more views and thus more votes. One confounder we investigate
 673 is periodicity in platform engagement across different weekdays. To investigate this, we analyze the
 674 average answer scores by weekday. As shown in Figure 1a, answers posted on Mondays receive
 675 significantly higher scores than those posted on Fridays. While one might speculate that this might
 676 be causal and reflect differences in writing quality, we observe a similar pattern in the average scores
 677 of questions themselves (Figure 1b), suggesting that broader engagement trends may be at play.

678 We further examine the number of views per question as a proxy for user exposure. Since the
 679 dataset does not include view counts for individual answers, we cannot directly assess the effect of
 680 exposure at the answer level. Figure 1c displays both question views and scores over time. The
 681 strong correlation between the two suggests that the observed temporal trends are more likely driven
 682 by fluctuations in user activity than by differences in content quality.

683 To test whether this bias can influence model behavior, we simulate a fine-tuning setup similar to that
 684 of Askell et al. (2021). We construct answer pairs based on user scores and designate the higher-
 685 scoring answer as preferred. For answers posted on Mondays, we prepend a neutral ‘‘Happy
 686 Monday! ’’ phrase to introduce a content marker correlated with engagement rather than quality. We then evaluate model generations on 3000 held-out questions and count how often the words
 687 ‘‘Happy’’ and ‘‘Monday’’ appear. Table 3 summarizes the results. The base pre-trained model rarely
 688 generates these terms. The supervised fine-tuned (SFT) should ideally capture the distribution in the
 689 data (generation temperature is set to 1). Our results show a frequency of $13.7\% \pm 0.2\%$ for the first
 690 word ‘‘Happy’’ which is consistent with the distribution in the data ($\sim 1/7$). In comparison, the DPO
 691 model generates ‘‘Happy’’ in $21.2\% \pm 0.8\%$ and ‘‘Monday’’ in $11.8\% \pm 0.8\%$, representing substan-
 692 tial increases of approximately 7.5 and 2.7 percentage points, respectively. To assess whether these
 693 increases are statistically significant, we perform independent two-sample t-tests over the 25 genera-
 694 tion rates from each model. The difference in ‘‘Happy’’ usage is highly significant ($p = 6.5 \times 10^{-10}$),
 695 and the increase in ‘‘Monday’’ usage is also statistically significant ($p = 3.4 \times 10^{-3}$). These results
 696 show that the model has internalized and amplified a spurious temporal signal. Additional details
 697 of this experiment, as well as further details about data and training characteristics, are provided in
 698 Appendix B.

699 This case highlights how confounding variables in observational datasets can lead to reward mis-
 700 specification and unintended behavior in fine-tuned models. Without accounting for causal struc-
 701 ture, models may learn to exploit spurious signals that correlate with success, even when they do not
 contribute to genuine task quality.

702 Table 3: Mean percentage (standard error) of generations containing “Happy” and “Monday” across
 703 5 generation seeds for the base model, and 25 runs (5 fine-tuning seeds \times 5 generation seeds) of SFT
 704 and DPO fine-tuning. DPO fine-tuning significantly amplifies the spurious weekday signal.

706 Model	707 Generations per Run	708 Num. Runs	709 With “Happy” (%)	710 With “Monday” (%)
707 Base Model	708 3000	709 5	710 1.13 (0.04)	711 0.07 (0.02)
707 SFT Model	708 3000	709 25	710 13.69 (0.21)	711 9.05 (0.19)
707 DPO Model	708 3000	709 25	710 21.22 (0.77)	711 11.78 (0.81)

712 **Data.** To replicate and extend the setup of Askell et al. (2021) we use data from the Academia
 713 Stack Exchange. The dataset contains 104,426 question-answer pairs. We retain only those ques-
 714 tions with multiple answers, reducing the data to 82,737 answer instances. To reduce memory usage
 715 during training, we further restrict to questions and answers with fewer than 180 words, yielding
 716 33,194 answers across 14,319 questions. Of these, 4,937 answers were written on a Monday.

717 We split the questions into three groups: 5,000 for supervised fine-tuning (SFT), 3,000 for testing,
 718 and the remainder for reward-based fine-tuning. For each question in the fine-tuning subset, we form
 719 ordered answer pairs by comparing scores and labeling the higher-scored answer as preferred. We
 720 cap the number of pairs per question at 10 to prevent imbalance. This yields 11,886 pairs, where we
 721 find a notable weekday skew: in pairs with only one Monday answer, 958 have the Monday answer
 722 as preferred, while 887 have it as rejected, hinting at temporal confounding.

723 **Fine-tuning setup.** We use the 360M parameter SmoLLM2-Instruct Allal et al. (2025) model
 724 as the base and perform two-stage fine-tuning.

725 **Supervised Fine-Tuning (SFT).** The SFT step uses the answer text as the assistant response and the
 726 corresponding question as input. Training is done for 1 epoch with a batch size of 8 and a learning
 727 rate of 2×10^{-4} using the AdamW optimizer (8-bit). We apply LoRA Hu et al. (2022) with rank 16
 728 and dropout 0.1. Inputs are tokenized using a custom prompt template with a 512-token sequence
 729 limit.

730 **Direct Preference Optimization (DPO).** The DPO stage initializes from the SFT checkpoint and
 731 fine-tunes using the constructed answer preference pairs. We use a β of 0.1 and train for up to 4
 732 epochs with a batch size of 8. LoRA is applied with rank 8. The maximum prompt and completion
 733 lengths are 256 and 512 tokens, respectively.

734 Generations for evaluation are performed on a held-out set of 3,000 questions, and model outputs
 735 are assessed for lexical artifacts. For the base model, which is fixed and not subject to any fine-
 736 tuning variability, we introduce randomness only through the generation process by using 5 different
 737 random seeds. In contrast, both the SFT and DPO models are subject to randomness in fine-tuning
 738 as well as generation. Specifically, we fine-tune each model using 5 different random seeds for
 739 initializing the model head, and then generate outputs from each trained model using 5 different
 740 generation seeds. This results in 25 runs per model, each producing 3000 generations.

741 To qualitatively assess the effect of fine-tuning, Table 4 presents representative generations from the
 742 base, SFT, and DPO models for a single held-out question. This example illustrates how fine-tuning
 743 shapes model behavior and provides evidence that the fine-tuning process is likely implemented
 744 correctly. The base model produces a generic answer formatted in Markdown (e.g., using `**` for
 745 bold), reflecting conventions likely present in its pretraining data. In contrast, the SFT model aligns
 746 more closely with the domain-specific formatting patterns found in the training set, namely, HTML
 747 tags. It adopts a tone more typical of answers on the target forum. The DPO model builds upon this,
 748 showing further alignment with patterns found in high-scoring answers: it employs richer format-
 749 ting (e.g., ``) and incorporates external references, likely reflecting learned associations
 750 between such features and answer quality.

751 **Compute.** All experiments for this setup were conducted on an NVIDIA RTX A6000 GPU. The
 752 Supervised Fine-Tuning (SFT) stage is relatively lightweight and completes in approximately 10
 753 minutes. In contrast, the Direct Preference Optimization (DPO) stage is more computationally in-
 754 tensive due to its iterative training on preference pairs and takes around 1 hour to run per seed.

Table 4: Comparison of model responses for a given question.

756	Question	Model	Generated Answer
759	"<p>I've been a Computer Sciences student for 4 years now, give or take, and my experience with emailing teachers/professors (teachers from now on) has been either of two cases: </p> they reply to my entire emailthey read the last sentence or paragraph and reply to that. <p>Generally, if a teacher fits in one of those categories, they always respond like that. However, for me it's quite frustrating to receive an email back (within 5 minutes, an hour, a day) with a reply, to only one point, and then having to mail back with my other questions, removing one question at a time.</p> <p>To note: my e-mails are always very respectful, neatly written, and without spelling or other mistakes.</p> <p>What can I do to get a higher percentage of questions-answered-per-email response?</p>"	760 761 762 763 764 765 766 767 768 769 770 771 772 773 774 775 776 777 778 779 780 781 782 783 784 785 786 787 788 789 790 791 792 793 794 795 796 797 798 799 800 801 802 803 804 805 806 807 808 809	757 Base Model 1. **Include specifics about the difficulties you face**: Instead of a general statement, explain the difficulties you're facing. This will show that you're willing to help by providing more details. 2. **Offer solutions to the problem**: Provide some strategies or tips to help teachers improve their email responses to your questions. This will show that you're proactive and interested in finding a solution to the problem. 3. **Provide clear examples of your goals and objectives**: Be specific about what you're trying to achieve by improving the response rate. For instance, you could say that you'd like to see more direct responses or more personalized responses from the teachers. 4. **Highlight any potential benefits to the school**: While you mentioned that the teacher-student ratio might be a problem, you could also mention that the improvement in response rate could positively affect the students, such as by having more individualized support. 5. **Emphasize the time and effort required**: Acknowledge that sending multiple emails back and forth might be time-consuming, but also express that the benefits of getting more responses are worth the extra effort. Example of how you could write a specific paragraph to demonstrate this: "I'm frustrated that I've received responses to my
810	811	812 SFT Model	813 <p>Happy Monday!</p><p>If my general attitude is that you should be able to reply to a very large number of emails with a single email, your teacher should answer the first few emails, since they don't need to spend a lot of time answering those.</p><p>On the other hand, if your teacher is very particular about your answers, you might want to offer more details about what you're trying to accomplish in your course, and what kind of questions you have and are trying to get answered.</p>
814	815	816 RL (DPO)	817 <p>Happy Monday!</p><p>The first point is that people generally answer more questions than they reply to in the course of an email. In a rough order, the answers are:</p>Less frequently, but they read the last sentence or paragraph and then reply to that: Reciprocity with you. It's nice to hear from you again and it's worth the extra effort for them to do so.Less frequently, but you read the last sentence or paragraph and then reply to that: Reciprocity.Ask a question and get answers.Less frequently, but you don't read the last sentence of paragraph and reply to that: <...>

810 **C UPWORTHY EXPERIMENT DETAILS**
 811

812 We follow a similar data processing approach to that of Ye et al. (2024), using the Upworthy dataset.
 813 The full dataset includes 150,817 headline-image “packages” across 32,487 A/B tests. Since some
 814 tests involve variation in both headlines and images, we restrict our analysis to headline-only tests
 815 where the image remains fixed. This filtering yields 17,682 headline-only tests comprising 77,245
 816 packages.

817 To construct the experimental dataset, we generate all possible headline pairs within each A/B test
 818 and retain only those with a statistically significant difference in click-through rate (CTR) at the 5%
 819 level. This results in 41,624 headline pairs covering 27,745 packages. We split these into training
 820 (60%), validation (20%), and test (20%) sets, while ensuring no headline appears in more than one
 821 split to avoid data leakage. The final dataset includes 24,842 training pairs, 8,395 validation pairs,
 822 and 8,387 test pairs.

823 These statistically significant pairs form the basis of our experimental setting. To simulate a non-
 824 experimental setting, we derive a corresponding observational dataset. For each headline test in the
 825 training set, we randomly retain only one package and discard the counterfactual. This results in
 826 8,499 training packages, representing approximately 26% of the total packages. This setup reflects
 827 a typical historical logging scenario, where only observed outcomes are available. Table 5 provides
 828 summary statistics of the experimental and observational datasets.

829 Before moving on to the modeling details, we briefly highlight a potential confounder that can affect
 830 observational CTRs: temporal variation in user engagement and topic salience. The probability that
 831 a user clicks on a given package depends not only on the quality or attractiveness of the headline,
 832 but also on who the viewers are and how relevant or important the topic is at the time. For instance,
 833 if a major sporting event occurs, the site may receive a surge of sports fans, whose preferences dis-
 834 proportionately influence overall CTRs. Similarly, politically themed headlines may receive more
 835 engagement during election periods. Figure 2a shows the average CTR by month for three data
 836 subsets: experimental training packages, observational training packages, and observational vali-
 837 dation packages. We observe a clear temporal pattern, with certain months getting substantially
 838 higher CTRs. Moreover, the CTR trends are highly correlated across subsets (pairwise correlations
 839 of monthly averages are between 96% and 97%), suggesting that these fluctuations are systematic
 840 rather than random.

841 This raises a concern for models trained directly on raw CTRs. They may overfit to superficial,
 842 time-related artifacts rather than learning meaningful properties of headline quality. As previously
 843 discussed, variations in CTR may partly reflect changes in the user population and taste rather than
 844 differences in content effectiveness. Figure 2b provides evidence of these changes, showing substan-
 845 tial variation in the number of impressions per package across months. Notably, there is a marked
 846 increase in impressions toward the end of 2023, coinciding with the U.S. election period. These
 847 fluctuations suggest that the volume and potentially the composition of website traffic change over
 848 time. As a result, shifts in user demographics or interests could introduce biases into the observed
 849 CTRs, potentially misleading models trained on such observational data.

850 **Reward modeling.** To train reward models, we use a prompting structure where the model is
 851 asked to generate a headline for a given news abstract:

852 System: You are an editor of a news website.
 853 Your task is to generate a headline for each news article that
 854 will attract the most readers. The headline should be less than 40 words.
 855 Only respond with the headline.
 856 User: The news abstract is '{lede}' News posted at {created_at}
 857 Assistant: {headline}

858 We use models from the Pythia suite Biderman et al. (2023) to generate embeddings, specifically
 859 extracting the representation of the final token in each output. A classification or regression head is
 860 added on top of this embedding to predict outcomes (CTR or preference), and an L_2 regularization
 861 parameter λ is tuned to manage overfitting, as detailed in the main text.

862 **Compute.** The most computationally intensive part of this experiment is generating embeddings
 863 using models from the Pythia suite. We extract the final-token representations, which serve as in-

864 Table 5: Summary statistics of the Upworthy dataset for experimental and observational settings.
865

Statistic	Upworthy Data	
	Experimental Data	Observational Data
Total headline-only A/B tests	17,682	–
Total packages	77,245	–
Statistically significant pairs	41,624	–
Packages in significant pairs	46,330	–
Training pairs	24,842	–
Training packages	27,745	7,285
Validation pairs	8,395	–
Validation packages	7,527	2,079
Test pairs	8,387	8,387

866 puts to the reward models. These embedding computations are performed on an AMD Radeon 7900
867 GPU. For the largest model used in our experiments, Pythia-12B, the embedding generation takes
868 approximately 12 minutes for the observational dataset and about 1.5 hours for the experimental
869 dataset, which is larger. Once embeddings are obtained, training the reward models with a classifi-
870 cation or regression head is relatively lightweight and runs efficiently on the Intel(R) Xeon(R) Gold
871 CPU @ 2.90GH.

872 D DETAILS OF SIMULATION EXPERIMENTS

873 For our synthetic experiments, we use the MIND (Microsoft News Dataset) (Wu et al., 2020), which
874 contains 160,000 English news articles, each with a headline and article body. To simulate user
875 engagement, we construct synthetic performance scores (interpretable as click-through rates) for the
876 article headlines using equations equation 3, equation 4, and equation 5. To find the sentiment of
877 each headline in the data, we use the sentiment analysis model from Yuan (2023).

878 To ensure domain consistency, we focus on the sports category, which includes 54,553 articles, the
879 largest among all categories. The data is split as follows: 20,000 articles for Supervised Fine-Tuning
880 (SFT), 10,000 for Reward Modeling (RM), 3,000 for reward validation, 10,000 for Proximal Policy
881 Optimization (PPO), and the rest for testing.

882 These synthetic scenarios allow us to explicitly test whether models can recover the true effect of
883 sentiment when the observed performance signal is partially corrupted by a structured confounder.

884 **Supervised Fine-Tuning.** We fine-tune a language model using SFT, where the model is prompted
885 to generate engaging headlines from article abstracts. The prompting structure is:

886 System: You are an editor of a news website. Your task is to
887 generate a headline for each news article that will attract the most
888 readers. The headline should be less than 30 words. Only respond with
889 the headline.
890 User: The news abstract is '{abstract}'
891 Assistant: {headline}

892 The base model is HuggingFaceTB/SmolLM2-360M-Instruct, fine-tuned with LoRA (rank
893 16, $\alpha=32$, dropout=0.1) for one epoch. We use a learning rate of $2e-4$ and batch size of 8.

894 **Reward modeling.** To train reward models on the synthetic performance scores, we perform hy-
895 perparameter tuning over several learning rates: { $2e-4$, $6e-4$, $8e-4$, $1e-3$, $2e-3$ }. Based on prior
896 findings (Ouyang et al., 2022), we limit training to one epoch to avoid overfitting.

918 **Generation results.** Table 1 summarizes the average sentiment of generated headlines and the
 919 frequency of team name mentions, which serve as a proxy for reliance on the popularity-based
 920 confounder. We discussed these results in Section 4.1.
 921

922 **Compute.** Our simulation experiments were run using two types of GPUs: NVIDIA RTX A6000
 923 and AMD Radeon 7900. For each combination of training seed and learning rate, reward modeling
 924 takes approximately 3–5 minutes on either GPU. However, the PPO fine-tuning stage is significantly
 925 more time-consuming, requiring about 2–3 hours to complete per setting.
 926

927 E IMPACTS AND ASSUMPTIONS OF OUR FRAMEWORK
 928

930 Our framework enables the use of observational data to align large language models (LLMs), thereby
 931 opening new possibilities for alignment with significant potential for positive social impact. As
 932 discussed in the main body of the paper, there are many real-world scenarios where conducting
 933 randomized experiments on content and messaging is infeasible, while firms often possess exten-
 934 sive historical observational data. In such cases, leveraging this data can substantially improve the
 935 alignment of LLMs with organizational or societal objectives. Consider, for example, a messaging
 936 system designed to improve medication adherence among patients. While running an experiment
 937 might be challenging due to engineering and ethical challenges, optimizing such a system using ob-
 938 servational data could lead to substantial improvements in health outcomes. However, as with any
 939 machine learning paradigm that seeks to optimize a performance metric, this approach also presents
 940 challenges. As highlighted in prior work Mehrabi et al. (2021), various forms of bias can influence
 941 the outputs of machine learning models.

942 Our framework specifically targets biases arising from confounders that influence both the treatment
 943 and the outcome. While we have not yet conducted empirical evaluations of the bias correction
 944 component with respect to mitigating group-level disparities, the proposed method can be used to
 945 account for societal factors that might otherwise lead a model to prefer one textual input over an-
 946 other based on irrelevant or unfair criteria. Furthermore, researchers and practitioners must consider
 947 heterogeneity in individual responses to different texts to prevent the model from unintentionally en-
 948 coding or amplifying structural disparities. For example, in a mobile health messaging application,
 949 if a particular message yields high adherence overall but performs poorly for a specific subgroup,
 950 it is crucial to incorporate recipient characteristics into the model to ensure equitable outcomes and
 951 avoid disproportionately favoring majority groups.

952 Turning to the theoretical underpinnings of our framework, prior work (see Section 2.3) often as-
 953 sumes that confounders have no effect on the outcome, implying a functional form $f(\mathbf{F}, \mathbf{C}) =$
 954 $f(\mathbf{F})$. However, this assumption may not hold in practice, especially in business settings where
 955 variables such as price are important drivers of outcomes. In contrast, our approach allows for a
 956 more realistic representation of the data-generating process, formulated as follows:

$$\begin{aligned} y_i &= f(\mathbf{X}_i) + \epsilon_i \\ &= f(T_i, \tilde{\mathbf{X}}_i) + \epsilon_i \\ &= g(T_i, \tilde{\mathbf{F}}_i) + h(\mathbf{C}_i) + \epsilon_i. \end{aligned} \tag{6}$$

957
 958
 959
 960
 961
 962 This formulation allows confounders to have a meaningful effect on outcomes, rather than assum-
 963 ing that outcomes are independent of confounder values. To ensure tractability, we impose two
 964 assumptions within our framework. First, we assume exogeneity of the error term conditional on the
 965 observed covariates, that is, $\mathbb{E}[\epsilon_i | \mathbf{X}_i] = 0$. This assumption is commonly made in empirical research
 966 involving high-dimensional covariates Zou & Zhang (2009), though it is not without limitations. As
 967 discussed in Fan & Liao (2014), even in high-dimensional settings, incidental or unintentional en-
 968 dogeneity can arise due to selection bias or model misspecification. Second, we assume a separable
 969 functional form in the final line of Equation 6, in which the effects of the confounders and the re-
 970 maining variables are additively decomposed. Importantly, the model remains flexible enough to
 971 capture interactions between g and h through their shared inputs, as illustrated in the entangled case
 972 described in Section 4.1.

972 While our framework introduces greater flexibility than prior approaches, we acknowledge the lim-
973 itations of these assumptions. The authors are currently working on developing a more general
974 framework that further relaxes these conditions.
975
976
977
978
979
980
981
982
983
984
985
986
987
988
989
990
991
992
993
994
995
996
997
998
999
1000
1001
1002
1003
1004
1005
1006
1007
1008
1009
1010
1011
1012
1013
1014
1015
1016
1017
1018
1019
1020
1021
1022
1023
1024
1025